Biological Trace Element Research (2024) 202:233–245
https://doi.org/10.1007/s12011-023-03667-3

RESEARCH

The Role of Glycogen Synthase Kinase-3β in the Zinc-Mediated Neuroprotective Effect of Metformin in Rats with Glutamate Neurotoxicity

Aykut Oruc[1] · Kadriye Yagmur Oruc[1,2] · Karolin Yanar[3] · Murat Mengi[4] · Aysel Caglar[5] · Bahar Ozturk Kurt[6] · Mehmet Altan[1] · Osman Fuat Sonmez[1] · Ufuk Cakatay[3] · Hafize Uzun[7] · Gonul Simsek[1]

Received: 8 March 2023 / Accepted: 11 April 2023 / Published online: 18 April 2023

Abstract

Metformin has been suggested to have protective effects on the central nervous system, but the mechanism is unknown. The similarity between the effects of metformin and the inhibition of glycogen synthase kinase (GSK)-3β suggests that metformin may inhibit GSK-3β. In addition, zinc is an important element that inhibits GSK-3β by phosphorylation. In this study, we investigated whether the effects of metformin on neuroprotection and neuronal survival were mediated by zinc-dependent inhibition of GSK-3β in rats with glutamate-induced neurotoxicity. Forty adult male rats were divided into 5 groups: control, glutamate, metformin + glutamate, zinc deficiency + glutamate, and zinc deficiency + metformin + glutamate. Zinc deficiency was induced with a zinc-poor pellet. Metformin was orally administered for 35 days. D-glutamic acid was intraperitoneally administered on the 35th day. On the 38th day, neurodegeneration was examined histopathologically, and the effects on neuronal protection and survival were evaluated via intracellular S-100β immunohistochemical staining. The findings were examined in relation to nonphosphorylated (active) GSK-3β levels and oxidative stress parameters in brain tissue and blood. Neurodegeneration was increased ($p < 0.05$) in rats fed a zinc-deficient diet. Active GSK-3β levels were increased in groups with neurodegeneration ($p < 0.01$). Decreased neurodegeneration, increased neuronal survival ($p < 0.01$), decreased active GSK-3β ($p < 0.01$) levels and oxidative stress parameters, and increased antioxidant parameters were observed in groups treated with metformin ($p < 0.01$). Metformin had fewer protective effects on rats fed a zinc-deficient diet. Metformin may exert neuroprotective effects and increase S-100β-mediated neuronal survival by zinc-dependent inhibition of GSK-3β during glutamate neurotoxicity.

Keywords Glutamate · GSK-3β · Metformin · Neurotoxicity · S-100β · Zinc

✉ Aykut Oruc
aykut.oruc@iuc.edu.tr

1 Department of Physiology, Cerrahpaşa Medical Faculty, Istanbul University-Cerrahpaşa, Istanbul, Turkey

2 Department of Physiology, Faculty of Medicine, Istinye University, Istanbul, Turkey

3 Department of Medical Biochemistry, Cerrahpaşa Medical Faculty, Istanbul University-Cerrahpaşa, Istanbul, Turkey

4 Department of Physiology, Medical Faculty, Namık Kemal University, Tekirdag, Turkey

5 Department of Pathology, Bagcilar Training and Research Hospital, Istanbul, Turkey

6 Department of Biophysics, Cerrahpaşa Medical Faculty, Istanbul University-Cerrahpaşa, Istanbul, Turkey

7 Department of Medical Biochemistry, Faculty of Medicine, Istanbul Atlas University, Istanbul, Turkey

Introduction

Metformin is an agent in the group of biguanide drugs used in the first-line treatment of prediabetes and type 2 diabetes. One of the main effects of metformin is to increase insulin receptor sensitivity [1] and regulate cellular energy homeostasis through adenosine monophosphate kinase (AMPK) activation [2]. Due to the positive effects of metformin on intracellular energy metabolism, it is thought that it has protective effects on the central nervous system (CNS), such as reducing the occurrence of postischemic damage [3], exerting neuroprotective effects during ischemia [4], and accelerating the recovery process after ischemic injury [5]. The basic mechanisms of these effects have not yet been clarified.

One of the intracellular mechanisms of insulin is the phosphorylation of insulin receptor substrate-1 (IRS-1) after insulin

receptor interactions. Phosphorylated IRS-1 (p-IRS-1) activates the phosphoinositide 3-kinase (PI3K)/Akt/mTOR pathway and causes cell proliferation through the inactivation of glycogen synthase kinase-3 beta (GSK-3β) by phosphorylating it at serine 9 [6, 7]. On the other hand, activation of GSK-3β stops cell proliferation through many mechanisms, creates insulin resistance, and initiates apoptosis by triggering oxidative stress and the activation of many proapoptotic genes, especially p53. The balance between GSK-3β activation and inhibition is important for cell survival [8]. Recent studies have shown that GSK-3β activity contributes to the pathogenesis of ischemic neuronal death [9], and GSK-3β inhibition protects against excitotoxicity [10]. Due to the dominant role of GSK-3β in neuronal apoptosis, modulating GSK-3β activity may be an important strategy to prevent ischemic neurodegeneration [9].

Similar effects of GSK-3β inhibition and metformin on the CNS suggest that metformin may exert its neuroprotective effects by inhibiting GSK-3β. However, there have been no adequate studies investigating the relationship between metformin and GSK-3β in the CNS.

Zinc is a vital ion that plays many roles in the body at physiological levels, such as reducing insulin resistance by activating IRS-1 [11], ensuring neuronal survival [12], and protecting against the toxic effects of glutamate through voltage-dependent and voltage-independent inhibition of N-methyl-D-aspartate (NMDA) receptors in the brain [13]. Similarly, it has been suggested that serum zinc levels are decreased in Alzheimer's disease compared to controls [14]. On the other hand, studies have shown that an increase in zinc ions in the cell inhibits GSK-3β [15].

S-100 calcium binding protein, also known as S-100β, is a member of the S-100 protein family and is found in the cytoplasm and nucleus of astrocytes and neurons [16]. While S-100β acts as a neurotrophic factor in the developing CNS, it plays an important role in glial and neuronal survival in the adult CNS [17]. It has been reported that the mechanisms responsible for neuronal survival include activating the PI3K/Akt/p21 pathway and reducing oxidative stress-related apoptosis by inhibiting GSK-3β [18, 19]. The relationship between S-100β and GSK-3β in neuronal survival is summarized in Fig. 1.

In this study, we investigated whether the effects of metformin on neuroprotection and neuronal survival were mediated by zinc-dependent inhibition of GSK-3β in rats with glutamate neurotoxicity. Neuronal survival was evaluated by examining intracellular S-100β levels, which are related to GSK-3β activation.

Materials and Methods

Study Design

Forty male, healthy, nongenetically modified, immunocompetent, 6- to 8-week-old *Sprague Dawley* rats (mean weight 300 ± 50 g) were obtained from Istanbul University Aziz Sancar Experimental Medicine Research Institute and included in the study. The use of female rats was avoided to rule out hormonal fluctuations due to menstrual cycles. During the experiment, each animal was housed in separate cages labeled with the experimental unit. Feeding and living conditions included a room temperature of 20–22 °C, an environment containing 55–60% humidity, and standard and low-zinc pellet feed on a 12-h daylight/12-h dark cycle. The zinc content of the standard pellet was 85 mg/kg, the nutritional content was 20% protein, 6% cellulose, and 2% fat, and the metabolizable energy value was 2600 kcal/kg. Low-zinc feed was specially produced (MBD Yem Ticareti, Gebze, Turkey) according to the "Altromin C 1040 Zinc deficiency diet" (Altromin International, Lage, Germany) formula. The zinc content was 4 mg/kg, and the other components were the same as the standard pellet. The experimental groups were created by block randomization of rats as follows:

I. Control (C) (n = 8)

The rats were fed standard pellets ad libitum and given a single daily dose of 3 ml of saline by gavage for 35 days. On the 35th day, 2.5 ml of saline was injected intraperitoneally.

II. Glutamate group (G) (n = 8)

The rats were fed standard pellets ad libitum and given a single daily dose of 3 ml of saline by gavage for 35 days. On the 35th day, 4 mg/kg D-glutamic acid was dissolved in 2.5 ml of saline and injected intraperitoneally.

III. Metformin + glutamate group (MG) (n = 8)

The rats were fed standard pellets ad libitum and given a single dose of 100 mg/kg metformin in 3 ml daily by gavage for 35 days. On the 35th day, 4 mg/kg D-glutamic acid was dissolved in 2.5 ml of saline and injected intraperitoneally.

IV. Zinc deficiency + glutamate group (ZG) (n = 8)

To induce zinc deficiency, the rats were fed a zinc-poor pellet (containing 5 mg/kg zinc) ad libitum and given a

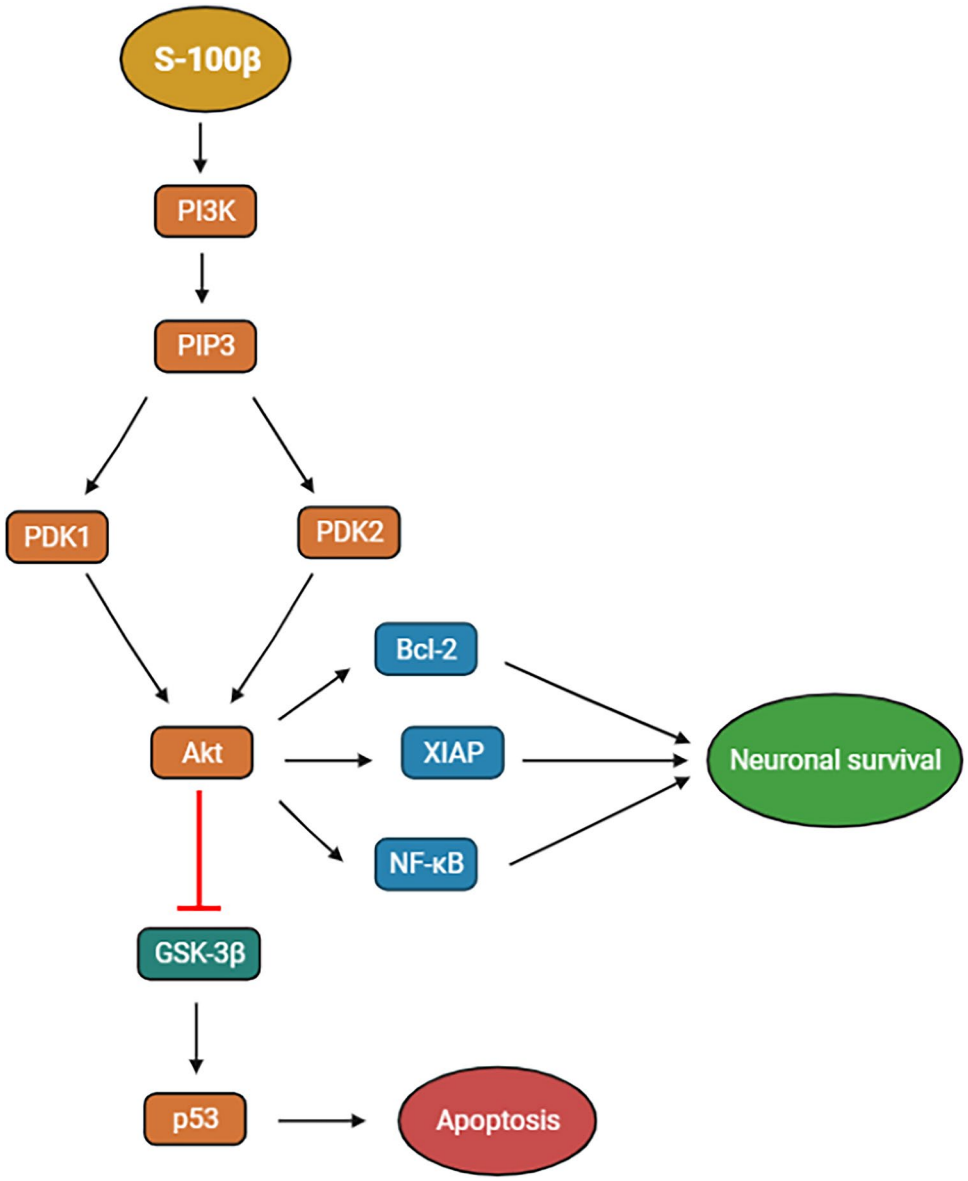

Fig. 1 Mechanism of the effect of intracellular S-100β on neuronal survival (created by Adobe Illustrator 27.2). Intracellular S-100β activates the PI3K/PIP3/Akt pathway, which inhibits stress-related apoptosis through the phosphorylation and tetramerization of p53 by inhibiting GSK-3β. The PI3K/PIP3/Akt pathway increases neuronal survival by activating Bcl-2, XIAP, and NF-κB during cellular stress. Pointed arrows show stimulation, blunt arrow shows inhibition. Abbreviations: PI3K, phosphoinositide 3-kinase; PIP3, phosphoinositide 3-kinase; PDK, phosphoinositide-dependent kinase; XIAP, X-linked inhibitor of apoptosis protein; NF-κB, nuclear factor kappa B; GSK-3β, glycogen synthase kinase-3 beta

single daily dose of 3 ml of saline by gavage for 35 days. On the 35th day, 4 mg/kg D-glutamic acid was dissolved in 2.5 ml of saline and injected intraperitoneally.

V. Zinc deficiency + metformin + glutamate group (ZMG) (n = 8)

To induce zinc deficiency, the rats were fed a zinc-poor pellet (containing 5 mg/kg zinc) ad libitum and given a single daily dose of 100 mg/kg metformin dissolved in 3 ml of saline by gavage for 35 days. On the 35th day, 4 mg/kg D-glutamic acid was dissolved in 2.5 ml of saline and injected intraperitoneally.

Gavage

The rats were gavaged with an 18-gauge metal feeding probe between 9:00 a.m. and 10:00 a.m. every day for 35 days. Metformin at a dose of 100 mg/kg was given to the MG and ZMG groups by gavage in a volume of 3 ml. The dose of metformin was selected considering the pharmacokinetics and oral bioavailability of metformin in rats. After calculating the intestinal and hepatic first-pass effects of metformin on rats, its oral bioavailability was stated to be 29.9% [20]. Considering this condition, the 100 mg/kg dose we planned to use in our study was close to 2550 mg/day, which is considered the upper limit of the maximum daily dose specified

by the Food and Drug Administration (FDA) in humans. When determining the 35-day administration period, studies showing that the neuroprotective effect of metformin occurred between 21 and 35 days for the shortest duration were taken into consideration [21, 22].

To rule out the effects of stress caused by gavage, rats in the other groups (C, G, ZG) were given 3 ml of saline by gavage for 35 days.

Intraperitoneal Injection

The rats were intraperitoneally injected in the lower abdominal outer quadrant on the 35th day. Rats in the G, MG, ZG, and ZMG groups were intraperitoneally injected after 4 mg/kg D-glutamic acid (powder) was dissolved in 2.5 ml of isotonic saline. The reason for using D-glutamic acid to create glutamate-induced neurotoxicity was that D-glutamic acid could not be deaminated in rats and could pass through the blood–brain barrier [23]. When determining the dose of D-glutamic acid for intraperitoneal administration, it was taken into consideration that the dose in question in the literature was the dose that caused convulsions but was considered to have a minimum mortality risk [23, 24].

To ensure that the stress caused by intraperitoneal injection did not affect the results of our study, 2.5 ml saline was administered to rats in the control group by intraperitoneal injection.

Collection of Blood and Tissue Samples

On the 38th day, 2 days after D-glutamic acid administration [25], an anesthetic combination of ketamine/xylazine (50 mg/kg/10 mg/kg) was intraperitoneally administered to the rats, and sacrifice was performed by hypovolemia caused by intracardiac blood collection. Blood samples were centrifuged at + 4 °C for 10 min, and serum was obtained. The frontal cortices and hippocampi, where glutamate neurotoxicity is intensely seen [26], were removed bilaterally from postmortem rats by paying attention to the cold chain, after which the samples were weighed, placed into tubes, and stored at − 80 °C. Right frontal cortex and hippocampus samples were marked numerically for blinding to reduce observer bias and collected for immunohistochemical and histopathological examinations. Left frontal cortex and hippocampus samples were turned into 20% tissue homogenates with the use of a glass homogenizer in ice molds using phosphate buffer (pH 7.4). Tissue homogenates were placed into previously labeled tubes and centrifuged at 5000 g at + 40 °C for 5 min. The resulting supernatants were divided into tubes, marked numerically for blinding to reduce observer bias, and stored in a deep freezer at − 80 °C until used.

Measurement of Nonphosphorylated (Ser9) GSK-3β Levels by ELISA

The nonphosphorylated (Ser9) GSK-3β ELISA kit was obtained from Aviva Systems Biology (MA, USA). The nonphosphorylated (Ser9) GSK-3β ELISA kit works on the basis of the enzyme immunoassay method using biotinylated nonphosphorylated (Ser9) GSK-3β antibodies and avidin-HRP conjugate. The supernatant was added to anti-nonphosphorylated GSK-3β-coated plates and incubated for 2 h at 37 °C. After the incubation period, the wells were emptied, and a biotinylated nonphosphorylated (Ser9) GSK-3-beta detector antibody was added. The wells were washed 3 times after being incubated at 37 °C for 1 h. Then, the wells were emptied and incubated with avidin-HRP conjugate for 1 h at 37 °C. After incubation, the wells were washed 5 times. Afterward, 3,3′,5,5′-tetramethylbenzidine (TMB) substrate was added to the wells and incubated for another 15 min. The enzyme–substrate reaction produced a blue-colored end-product. Finally, the blue-colored product turned yellow when the stop solution was added to stop the reaction. The optical density of the colored product was measured spectrophotometrically at 540 nm in an optical reader. The nonphosphorylated (Ser9) GSK-3β concentration of each sample was calculated based on the standard curve.

Measurement of Zinc Levels

Zinc levels in acid-dissolved frontal cortex and hippocampus tissues and serum were measured in a Thermo iCAP 600 series inductively coupled plasma optical emission spectrophotometer (ICP–OES) (Thermo Fisher, MA, USA) at a wavelength of 206 nm.

Pathological Examinations

Histopathology

After the brain tissues were fixed in 20 ml of 10% formalin for 24 h, macroscopic sections including the cortical and subcortical tissues of the frontal and temporal lobes were prepared. Paraffin blocking was then performed. Nissl staining was performed on each block by preparing 4 µm sections. The covering solution was added to the stained slides and covered with a coverslip. To evaluate Nissl staining, the rate of degenerated cells was determined in three fields in cortical and subcortical areas using × 40 and × 100 objectives and Image-Pro Plus 7 software (Media Cybernetics, MD, USA).

Immunohistochemistry

Sections with a thickness of 4 μm were obtained from paraffin blocks and prepare on slides previously coated with poly-L-lysine. The sections were kept in an oven at 56 °C overnight. The EP32 clone of the S-100β antibody was used for immunohistochemical staining and was obtained from Cell Marque (CA, USA), and the secondary Bond Polymer Refine 3,3′-Diaminobenzidine (DAB) kit was obtained from Leica (Newcastle, UK). Staining was completed by incubating the samples in S-100β immunohistochemical stain at a 1:400 dilution in Leica Bond Max IHC Stainer (Leica, Newcastle, UK) for 32 min.

An Olympus BX51 light microscope (Tokyo, Japan) was used for the examination.

Nuclear staining at any level was considered immunoreactive in the immunohistochemical evaluation of S-100β. Cells with immunoreactivity in three areas in the cortical and subcortical areas were determined using × 40 and × 100 objectives. Then, using the × 400 objective, cells with a positive nuclear reaction among a total of 100 cells were detected, and the number of positively stained cells in 100 cells was determined.

Biochemical Colorimetric Analytical Methods

Advanced Oxidation Protein Products

Analysis of advanced oxidation protein product (AOPP) levels was performed on serum and brain homogenates by modifying the spectrophotometric method of Hanasand et al. [27].

Malondialdehyde

Serum and brain homogenates were used to determine malondialdehyde (MDA) levels. MDA reacts with thiobarbituric acid (TBA) to form a colored product with a maximum absorbance at 535 nm. The efficiency of lipid peroxidation was examined with the colorimetric method described by Buege and Aust [28].

Lipid Hydroperoxides

Lipid hydroperoxide levels in serum and brain homogenates were calculated via the colorimetric method described by Jiang et al. [29]. In the presence of lipid hydroperoxides (L-OOH), ferrous (Fe^{+2}) ions in an acidic medium are oxidized to ferric (Fe^{+3}) ions. The ferric ions form a one-to-one, colored, soluble complex (blue–violet) with ferric xylenol orange 2 (FOX2). The absorbance of the supernatant fraction was read at 560 nm against a reagent blank. $\varepsilon = 4.46 \pm 0.23 \times 104\ M^{-1}\ cm^{-1}$ was used as the molar extinction coefficient in the calculations.

Analysis of Protein-Bound Advanced Glycation End-Products

Analysis of protein-bound advanced glycation end-products (AGEs) in serum and brain homogenates was performed according to the spectrofluorimetric method. To prevent fluorescence interference, the samples were pretreated according to the method described by Yanar et al. [30]. In the next step, protein-containing pellets were dissolved in 6 M guanidine-HCl, and fluorescence values were measured [30]. The fluorescence intensities of the samples at an excitation of 350 nm and maximum emission at 440 nm were recorded. The fluorescence intensity is expressed as FU/mg protein.

Cu–Zn Superoxide Dismutase Activity

Cu–Zn superoxide dismutase (SOD) (EC 1.15.1.1) activity in serum and brain homogenates was determined by the method described by Sun and Oberley [31]. The absorbance value was read at 560 nm against a reagent blank. One unit of Cu–Zn SOD is defined as the enzyme activity that dismutes the superoxide radical anion by 50%.

Catalase Activity

Catalase (CAT) activity (E.C.1.11.1.6) in serum was determined according to the method described by Aebi [32]. The degradation rate of H_2O_2 was observed kinetically at 240 nm. Then, 750 μL of PBS containing 30 mM H_2O_2 was added to 10 μL of the sample, and the change in absorbance was recorded for 1 min. The molar absorptivity value of 43.6 $M^{-1}\ cm^{-1}$ was used to calculate the activity. One unit of catalase is defined as 1 μmol H_2O_2 broken down per minute, and CAT activity is expressed as U/mg protein.

Evaluation of Total Protein Levels

Measurement of protein levels in brain homogenates was performed fluorometrically with a Qubit analyzer (Invitrogen, Carlsbad, CA). The absorbance of the purple color formed in the samples was measured at 550 nm. The protein concentration of the samples was calculated with the standard curve formed by different concentrations of albumin solutions (2.5–80 mg/ml) prepared by serial dilution.

Statistical Analysis

Statistical analysis was performed using the Statistical Package of Social Sciences (SPSS) program (SPSS Inc.: IL, USA,

version 12.0). According to the results of the power analysis (mean 10 units difference and 5 units standard deviation at 80% power and 95% confidence level), it was determined that a minimum of 8 rats were required for each group. The Kolmogorov–Smirnov test was used to determine the normality distribution of the data. Parametric or nonparametric tests were selected according to the number of groups, normality distribution, and homogeneity (M: 50, SD: 10 at 95% CI). Nonparametric tests were used because our data did not fit the normality distribution. Pairwise comparisons between groups were made using the Mann–Whitney *U* test. The analysis of numerical data for which the standard deviation could not be calculated was performed using a one-sample *t* test. A value of $p < 0.05$ was considered significant for all statistical analyses. The data are expressed as the mean ± standard deviation.

Results

Zinc Levels

Zinc levels in serum and brain tissue were significantly lower in the zinc-poor diet groups (ZM and ZMG) than in the other groups ($p < 0.05$) (Fig. 2).

Active GSK-3β Levels

Nonphosphorylated (Ser9) GSK-3β levels in serum and brain tissue were significantly higher in the G group than in the control group ($p < 0.01$), and zinc deficiency increased active GSK-3β levels even more when the G group was compared to the ZG group ($p < 0.01$). Comparing the MG group to the G group and the ZMG group to the ZG group, it was observed that metformin significantly prevented the increase in GSK-3β levels ($p < 0.01$). However, when the ZMG and MG groups were compared, GSK-3β levels were higher in the ZMG group ($p < 0.05$), and so the effect of metformin was alleviated by zinc deficiency (Fig. 3).

S-100β Staining Rates

Cortical and hippocampal intracellular S-100β staining rates were significantly higher in the G group than in the control group ($p < 0.05$) due to increased survival. However, zinc deficiency negatively affected hippocampal and cortical neuronal survival when the G group was compared to the ZG group ($p < 0.05$). Comparing the MG and G groups, it was observed that metformin administration significantly increased intracellular S-100β staining rates in cortical and hippocampal neurons ($p < 0.01$). However, the staining rates of hippocampal and cortical neurons were significantly lower in the ZMG group than in the MG group ($p < 0.01$ and $p < 0.001$, respectively), showing that the effect of metformin on survival was alleviated by zinc deficiency (Figs. 4, 5, and 6).

Neurodegeneration Rates

Degenerated cortical and hippocampal neuron rates were significantly higher in the G group than in the C and MG groups, as shown by Nissl staining ($p < 0.01$). When comparing the ZG group to the G group and the ZMG group to the ZG group, zinc deficiency significantly increased neuronal degeneration rates ($p < 0.05$ and $p < 0.01$, respectively). On the other hand, neurodegeneration rates were significantly lower in the hippocampal and cortical areas in the MG group than in the G group ($p < 0.01$ and $p < 0.001$, respectively).

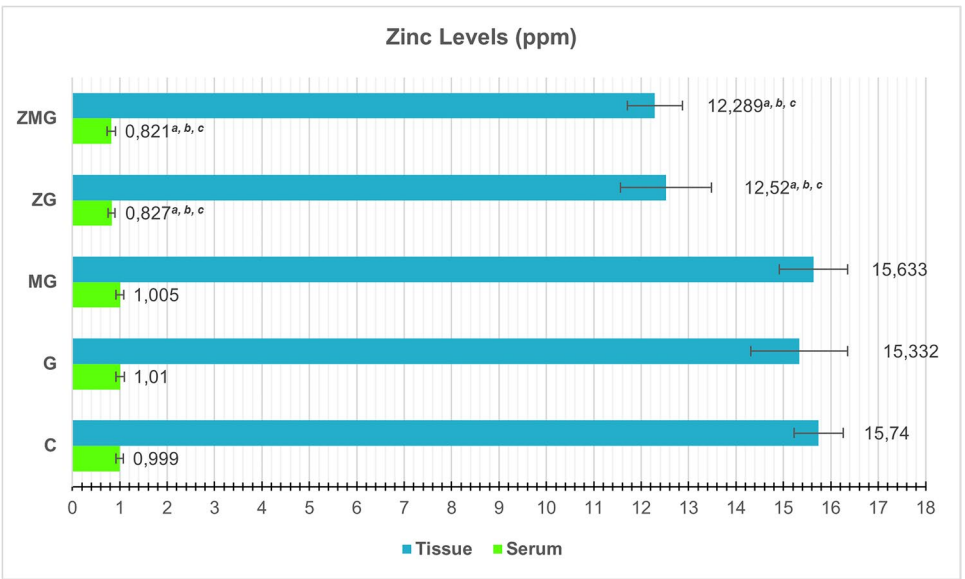

Fig. 2 Serum and tissue zinc levels. Values are expressed as the means ± SD. The letters indicate significant differences ($p < 0.05$): [a]C; [b]G; [c]MG. (%95 CI). Abbreviations: C, control; G, glutamate; MG, metformin + glutamate; ZG, zinc deficiency + glutamate; ZMG, zinc deficiency + metformin + glutamate; ppm, parts per million

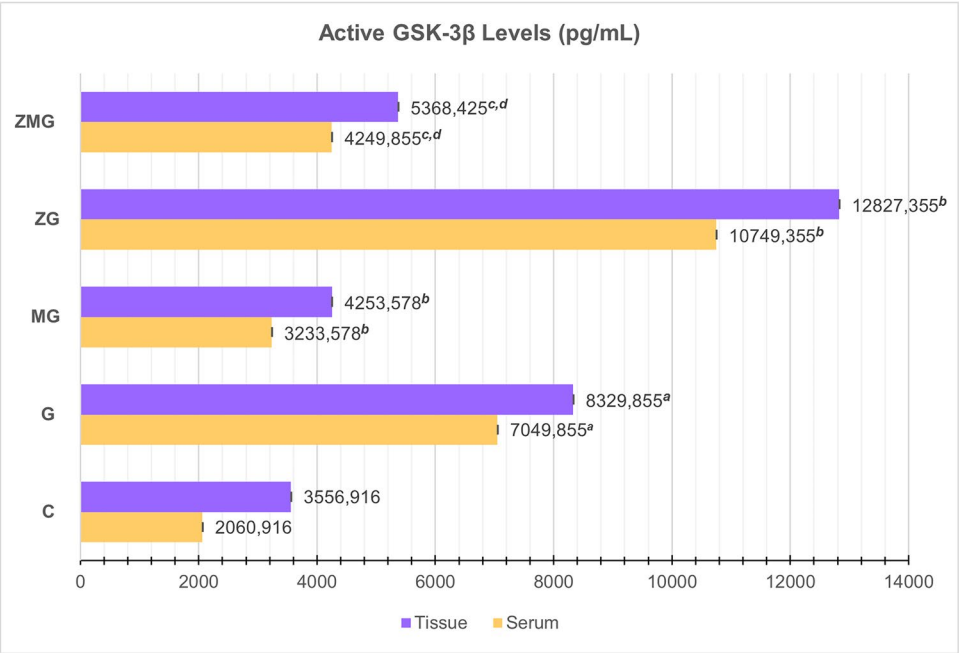

Fig. 3 Serum and tissue levels of active GSK-3-beta. Values are expressed as the means ± SD. The letters indicate significant differences ($p < 0.01$): [a]C; [b]G; [c]MG ($p < 0.05$): [d]ZMG. (%95 CI). Abbreviations: C, control; G, glutamate; MG, metformin + glutamate; ZG, zinc deficiency + glutamate; ZMG, zinc deficiency + metformin + glutamate; GSK-3β, glycogen synthase kinase 3-β

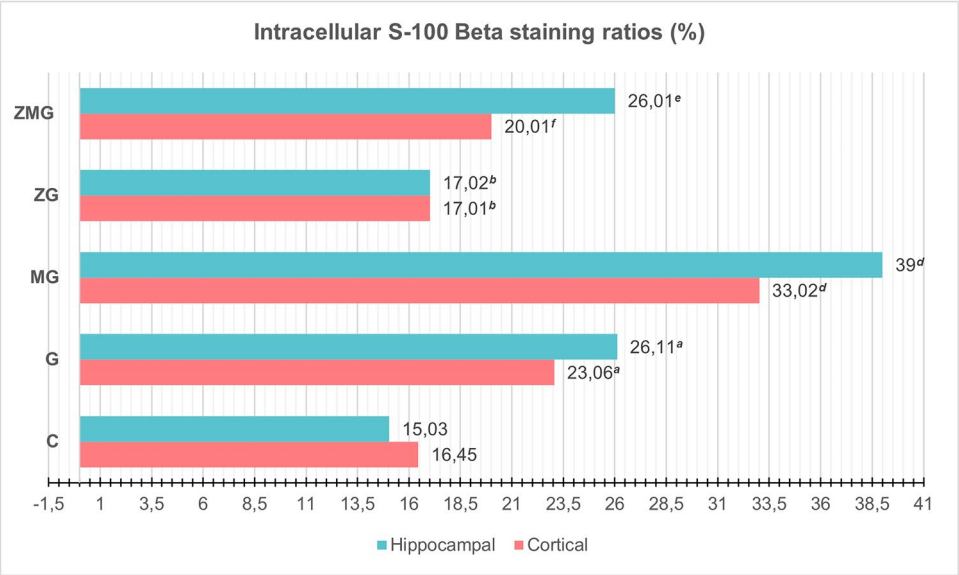

Fig. 4 Cortical and hippocampal intracellular S-100 beta staining ratios (%). Values are expressed as the means. The letters indicate significant differences ($p < 0.05$): [a]C; [b]G; [c]ZG ($p < 0.01$): [d]G; [e]MG ($p < 0.001$): [f]MG. (%95 CI). Abbreviations: C, control; G, glutamate; MG, metformin + glutamate; ZG, zinc deficiency + glutamate; ZMG, zinc deficiency + metformin + glutamate

Metformin did not exert its effects strictly in the context of zinc deficiency, and the neurodegeneration rates were significantly higher in the ZMG group than in the MG group ($p < 0.01$) (Fig. 7).

Biochemical Colorimetric Analytical Methods

Advanced Oxidation Protein Products and Protein-Bound Advanced Glycation End-Products

AOPP and AGE levels in serum were significantly higher in the G group than in the C group ($p < 0.05$ and $p < 0.01$, respectively). Zinc deficiency increased serum AOPP levels even more when the ZG group was compared to the G group ($p < 0.05$), but serum AGE levels were unaffected when the ZG group was compared to the G group ($p > 0.05$). Metformin administration decreased serum AOPP and AGE levels in the context of glutamate toxicity when the MG group was compared to the G group ($p < 0.01$ and $p < 0.05$, respectively). However, this effect of metformin was not observed in the context of zinc deficiency. Serum AOPP and AGE levels were significantly higher when the ZMG group was compared to the MG group ($p < 0.01$) (Fig. 8).

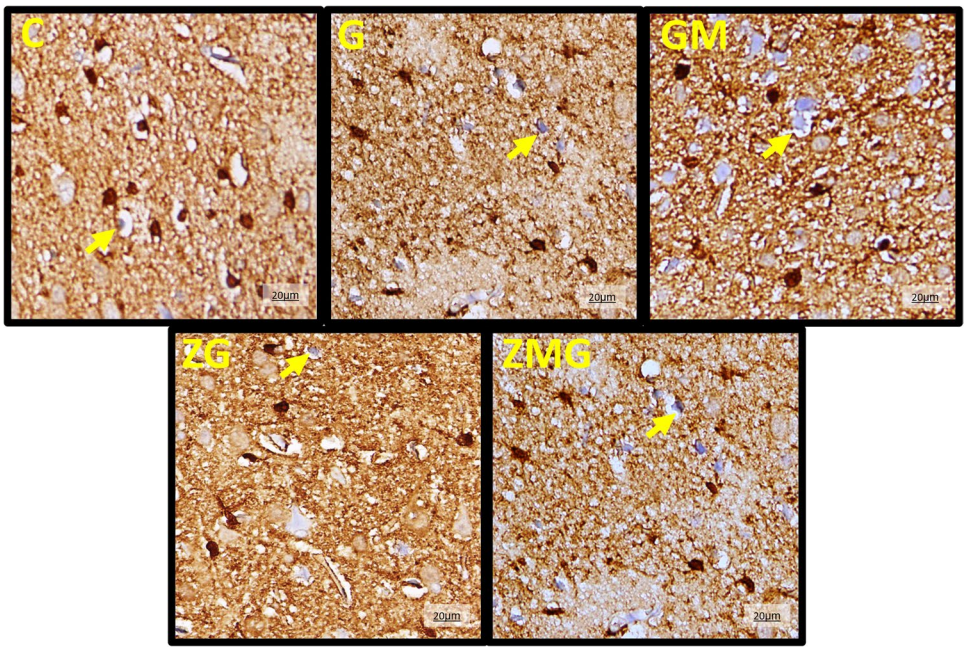

Fig. 5 Cortical multipolar neuron samples were immunohistochemically stained for S-100β. Images were taken at 400 × magnification and randomly selected from among the groups. The tips of the yellow arrow indicate S-100β-stained cells. Abbreviations: C, control; G, glutamate; GM, metformin + glutamate; ZG, zinc deficiency + glutamate; ZMG, zinc deficiency + metformin + glutamate

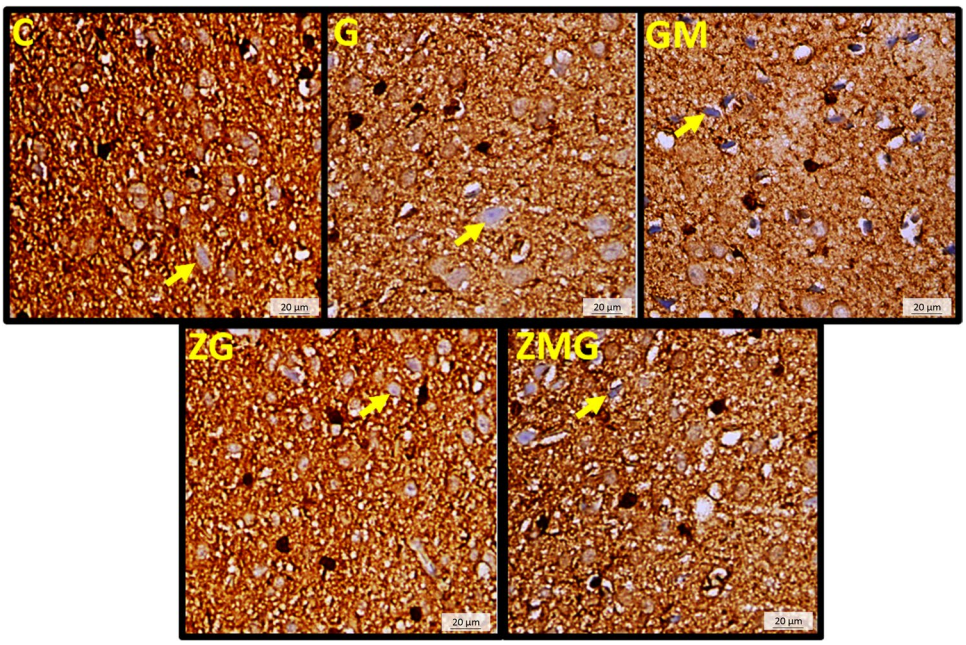

Fig. 6 Hippocampal multipolar neuron samples were immunohistochemically stained for S-100β. Images were taken at 400 × magnification and randomly selected from among the groups. The tips of the yellow arrow indicate S-100β-stained cells. Abbreviations: C, control; G, glutamate; GM, metformin + glutamate; ZG, zinc deficiency + glutamate; ZMG, zinc deficiency + metformin + glutamate

As shown in Fig. 8, changes in tissue AOPP levels were equivalent to changes in serum levels in all groups. However, there was no significant difference in tissue AGE levels between the groups (Fig. 8).

Antioxidant Enzyme Activities and Other Oxidation Products

As shown in Fig. 9, glutamate toxicity increased serum MDA and L-OOH levels and decreased Cu–Zn-SOD and CAT activity when the G group was compared to the control group. On the other hand, zinc deficiency induced no significant changes in these serum markers when the ZG group was compared to the G group ($p > 0.05$). Metformin decreased serum MDA and L-OOH levels and Cu–Zn-SOD and CAT activity when the MG group was compared to the G group. However, metformin could not exert this effect in the context of zinc deficiency, and serum MDA and L-OOH levels were significantly increased, while serum Cu–Zn-SOD and CAT activities were significantly decreased when the ZMG group was compared to the MG group (Fig. 9).

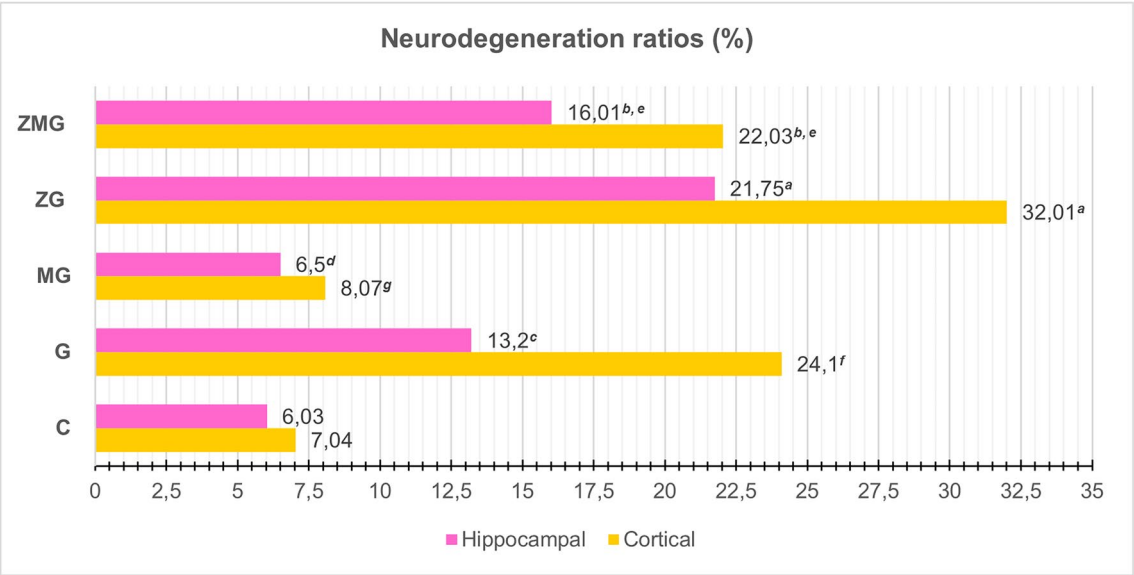

Fig. 7 Cortical and hippocampal neurodegeneration ratios (%). Values are expressed as the means. The letters indicate significant differences ($p<0.05$): [a]G; [b]ZG; [c]C ($p<0.01$): [d]G; [e]MG ($p<0.001$): [f]C; [g]G. (%95 CI). Abbreviations: C, control; G, glutamate; MG, metformin + glutamate; ZG, zinc deficiency + glutamate; ZMG, zinc deficiency + metformin + glutamate

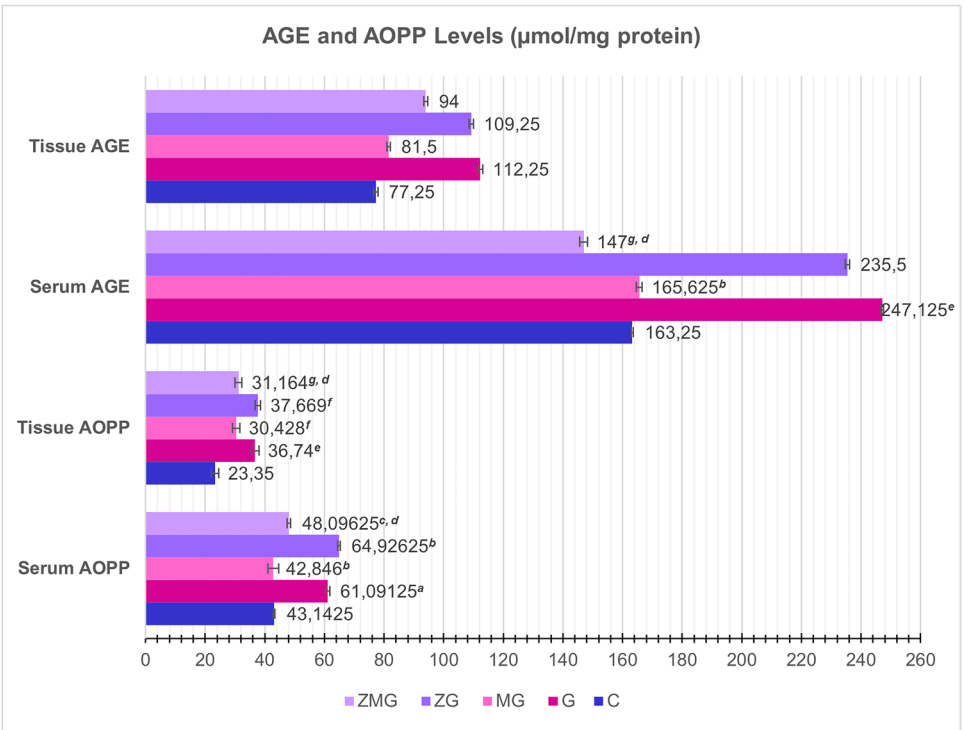

Fig. 8 AGE and AOPP levels. Values are expressed as the means ± SD. The letters indicate significant differences ($p<0.05$): [a]C; [b]G; [c]ZG ($p<0.01$): [d]MG; [e]C, [f]G. (%95 CI). Abbreviations: C, control; G, glutamate; MG, metformin + glutamate; ZG, zinc deficiency + glutamate; ZMG, zinc deficiency + metformin + glutamate; AOPP, advanced oxidation protein products; AGE, protein-bound advanced glycation end-products

As shown in Fig. 9, the changes in tissue MDA and L-OOH levels were parallel to the changes in serum levels in all groups. However, there was no significant difference in tissue Cu–Zn-SOD activity between the groups. Measurement of catalase activity in tissue samples could not be performed due to technical problems.

Discussion

Our research shows that metformin protects against neuronal damage caused by glutamate. This neuroprotective effect is mediated by zinc-dependent inhibition of GSK-3β.

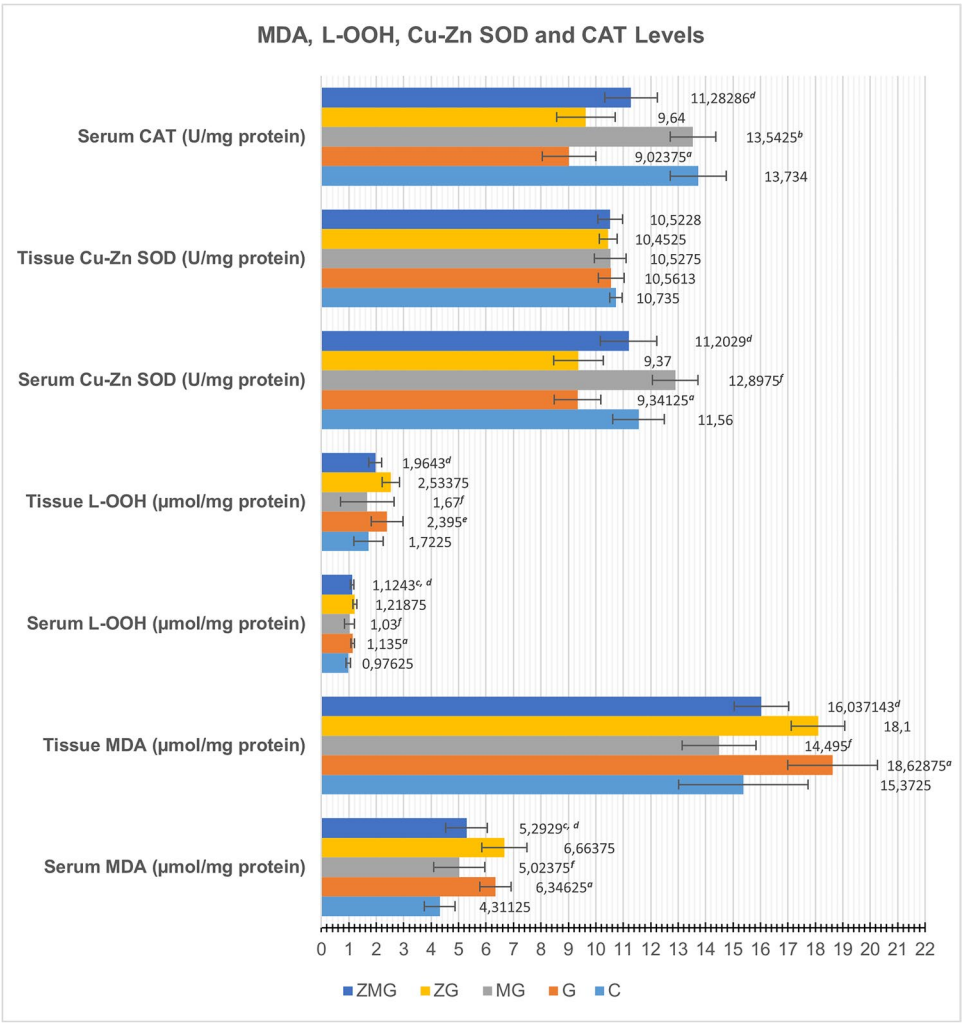

Fig. 9 MDA, L-OOH, Cu–Zn SOD, and CAT levels. Values are expressed as the means ± SD. The letters indicate significant differences ($p < 0.05$): ^{a}C; ^{b}G; ^{c}ZG ($p < 0.01$): ^{d}MG; ^{e}C, ^{f}G. (%95 CI). Abbreviations: C, control; G, glutamate; MG, metformin + glutamate; ZG, zinc deficiency + glutamate; ZMG, zinc deficiency + metformin + glutamate; MDA, malondialdehyde; L-OOH, lipid hydroperoxide; SOD, superoxide dismutase; CAT, catalase

Our histopathological findings indicate that significant damage occurs in the cortical and hippocampal regions of rats administered D-glutamic acid. It was concluded that the neuronal degeneration caused by D-glutamic acid was even more prominent in rats with zinc deficiency (Fig. 7), which is consistent with previous studies [14, 33, 34]. Some studies have reported that zinc inhibits NMDA receptors [35, 36] and glutamate release [37, 38] by interacting with the zinc-binding site on postsynaptic and presynaptic receptors, respectively. Thus, the disappearance of NMDA receptor inhibition and the increase in glutamate secretion from presynaptic neurons in the context of zinc deficiency may be responsible for the increased damage in the cortical and hippocampal regions of rats fed a zinc-deficient diet. Additionally, Ilouz et al. showed that an increase in zinc in the cell inhibits GSK-3β [15]. The occurrence of similar events during zinc deficiency and GSK-3β activation may be related to an increase in GSK-3β activity in the context of zinc deficiency.

In our study, there were significant increases in active GSK-3β levels in the blood and brain tissue of rats in groups with D-glutamic acid-induced neurodegeneration (G and ZG). Similarly, Hanumanthappa et al. suggested that GSK-3β plays a role in brain damage by increasing glutamate secretion as a result of ischemia [9].

Our research suggests that metformin has a neuroprotective effect by inhibiting GSK-3β activity in neurodegeneration caused by glutamate increase. Our histopathological findings revealed that glutamate-induced neurodegeneration (Fig. 7) and active GSK-3β levels were significantly reduced (Fig. 3) in the metformin-treated groups compared to the untreated groups. Similarly, Leng et al. showed that inhibiting GSK-3β protected against cerebral ischemia and prevented glutamate-induced neurodegeneration [39, 40]. Cross et al. showed that inhibiting GSK-3β weakened apoptotic signals and prevented neuronal death [41].

In addition, intracellular S-100β staining rates, which are indicators of neuronal survival and regeneration, were

higher in the G group than in the control group (Fig. 4). Considering the neurodegeneration rates in the same groups (Fig. 7), this finding shows us that neurons damaged due to glutamate toxicity begin to regenerate. In addition, although the intracellular S-100B staining rates in the ZG group were higher than those in the C group, there was no statistically significant difference, indicating that this regeneration was restricted by zinc deficiency. On the other hand, intracellular S-100β staining rates were higher in the metformin-treated groups (MG, ZMG) than in the untreated groups (G, ZG), suggesting the positive effect of metformin on neuronal survival (Fig. 4). Our findings also revealed that these protective effects of metformin on neurons were lower in groups fed a zinc-deficient diet than in groups fed a normal diet (Fig. 4). These findings suggest that metformin inhibits GSK-3β not only through the AMPK-Akt pathways but also through zinc-dependent pathways. Similarly, Miranda et al. suggested that IRS-1 phosphorylation, which causes Akt activation, may occur not only through AMPK but also directly through intracellular zinc [42]. Metformin may cause zinc to contribute to IRS-1 phosphorylation at this stage. Therefore, the decrease in intracellular zinc levels in rats fed a zinc-deficient diet may be responsible for the reduced protective effects of metformin. On the other hand, S6K, a zinc-dependent protein kinase, has been reported to inhibit GSK-3β in some studies and can cause activation in other studies [43, 44]. It has been suggested that the effect of S6K on GSK-3β may differ between tissues [45]. We think that metformin can inhibit GSK-3β by directly increasing S6K expression in the CNS. Further studies are needed to investigate the effect of metformin on the expression or activation of S6K and its relationship with GSK-3β.

In our study, the increase in blood AGE levels in D-glutamic acid-administered rats was notable. Huang et al. stated that increased glutamate could impair the function of β-cells and accelerate their apoptosis through the overactivation of NMDA receptors [46]. Additionally, Shen et al. suggested that inhibition of GSK-3β induces human pancreatic β-cell proliferation [47]. Consistent with this information, overstimulation of NMDA receptors in pancreatic beta cells may be responsible for the increase in blood AGE levels by increasing active GSK-3β levels in D-glutamic acid-administered rats.

AGEs activate reactive oxygen species (ROS) and advanced glycation end-product receptors (AGERs), which produce an inflammatory response [48]. This interaction between AGERs and AGEs causes increases the synthesis of the superoxide radical anion. This reduces the activity of catalase and superoxide dismutase [48]. We think that the decrease in Cu–Zn SOD and catalase activities in the blood of D-glutamic acid-administered rats may have developed due to the increased use of these antioxidants to remove the increased ROS in peripheral tissues.

Our findings suggest that the increase in oxidative stress observed in glutamate-administered rats (G, ZG) may be related to the increase in active GSK-3β levels (Figs. 3, 8, and 9). Similarly, Li et al. reported that GSK-3β increases ROS formation by causing mitochondrial dysfunction in neurons [49]. On the other hand, oxidative stress parameters such as AGE, AOPP, MDA, and L-OOH in serum and tissue were significantly decreased in rats treated with metformin (GM, ZGM) compared to untreated rats (G, ZG). There were also significant increases in serum Cu–Zn SOD and catalase activities in the metformin-treated groups (Figs. 8, 9). These results suggest that the protective effects of metformin are due to decreasing ROS production and regulating the balance between pro-oxidants and antioxidants. These findings are consistent with other studies suggesting that metformin has a similar effect on other tissues [50, 51]. Similarly, Zhao et al. suggested that metformin treatment provided cognitive protection in mice with pentylenetetrazole (PTZ)-induced epilepsy models and showed antioxidant effects by reducing oxidative stress [52].

Finally, our findings showed that metformin administration to rats fed a zinc-deficient diet did not reduce lipid peroxidation caused by glutamate toxicity in brain tissue. This shows us that metformin needs zinc to prevent glutamate-induced lipid peroxidation, especially in brain tissue.

In conclusion, our study is the first to investigate the relationship of metformin with GSK-3β and zinc in the brain. We can say that the increase in glutamate secretion may cause an increase in oxidative stress via GSK-3β. Our findings confirm that metformin can inhibit glutamate-mediated neurodegeneration and increase neuronal survival by reducing active GSK-3β levels through zinc-dependent pathways. Further studies are needed to investigate the advanced intracellular pathways metformin by which affects GSK-3β in brain tissue.

Limitations

While planning this study, we aimed to fill the gaps in the mechanism of the neuroprotective effect of metformin, which is still not fully understood, and to show whether zinc has a role in these mechanisms. Both for this reason and to keep the number of animals less for ethical reasons, we did not examine the effects of the zinc deficiency group alone on all parameters. Similar studies to be conducted in the future will contribute to the literature to examine the effects of zinc deficiency on the parameters we investigated in our study. Also, we could not measure catalase activity in tissue samples due to technical problems during storage, but considering the other results, we think that the results of the tissue samples would be consistent with the results obtained from the serum samples.

Author Contribution All authors contributed significantly to this research.

Conceived and designed the experiments and wrote the manuscript: AO, GS. Performed the experiments and analyzed the data: AO, KYO, KY, MM, MA, AC, BOK, OFS, UC, HU, GS. The corresponding author: AO. All authors have been involved in the drafting, critical revision, and final approval of the manuscript for publication. All authors agree to be accountable for all aspects of the work in ensuring that questions related to the accuracy or integrity of any part of the work are appropriately investigated and resolved.

Funding This study was funded by the Istanbul University Scientific Research Projects. Project No: 27509.

Data Availability The raw data supporting this study will be available by authors to any qualified researcher upon request.

Declarations

Ethics Approval Ethical approval was obtained for the project from Istanbul University Animal Experiments Local Ethics Committee with the number 35980450–050.99. Guide for the Care and Use of Laboratory Animals of National Academy of Sciences was followed for caring animals during the experiment.

Competing Interests The authors declare no competing interests.

References

1. Collier CA, Bruce CR, Smith AC, Lopaschuk G, Dyck DJ (2006) Metformin counters the insulin-induced suppression of fatty acid oxidation and stimulation of triacylglycerol storage in rodent skeletal muscle. Am J Physiol Endocrinol Metab 291(1): E182–E189. https://doi.org/10.1152/ajpendo.00272.2005
2. Russo GL, Russo M, Ungaro P (2013) AMP-activated protein kinase: a target for old drugs against diabetes and cancer. Biochem Pharmacol 86(3):339–350. https://doi.org/10.1016/j.bcp.2013.05.023
3. Ashabi G, Khalaj L, Khodagholi F, Goudarzvand M, Sarkaki A (2015) Pre-treatment with metformin activates Nrf2 antioxidant pathways and inhibits inflammatory responses through induction of AMPK after transient global cerebral ischemia. Metab Brain Dis 30(3):747–754. https://doi.org/10.1007/s11011-014-9632-2
4. Jiang T, Yu JT, Zhu XC, Wang HF, Tan MS, Cao L, Zhang QQ, Gao L, Shi JQ, Zhang YD, Tan L (2014) Acute metformin preconditioning confers neuroprotection against focal cerebral ischaemia by pre-activation of AMPK-dependent autophagy. Br J Pharmacol 171(13):3146–3157. https://doi.org/10.1111/bph.12655
5. Jin Q, Cheng J, Liu Y, Wu J, Wang X, Wei S, Zhou X, Qin Z, Jia J, Zhen X (2014) Improvement of functional recovery by chronic metformin treatment is associated with enhanced alternative activation of microglia/macrophages and increased angiogenesis and neurogenesis following experimental stroke. Brain Behav Immun 40:131–142. https://doi.org/10.1016/j.bbi.2014.03.003
6. Sutherland C, Leighton IA, Cohen P (1993) Inactivation of glycogen synthase kinase-3 beta by phosphorylation: new kinase connections in insulin and growth-factor signalling. Biochem J 296(Pt 1):15–19. https://doi.org/10.1042/bj2960015
7. Grabinski T, Kanaan NM (2016) Novel non-phosphorylated serine 9/21 GSK3β/α antibodies: expanding the tools for studying GSK3 regulation. Front Mol Neurosci 9:123. https://doi.org/10.3389/fnmol.2016.00123
8. Watcharasit P, Bijur GN, Zmijewski JW, Song L, Zmijewska A, Chen X, Johnson GV, Jope RS (2002) Direct, activating interaction between glycogen synthase kinase-3beta and p53 after DNA damage. Proc Natl Acad Sci USA 99:7951–7955. https://doi.org/10.1073/pnas.122062299
9. Hanumanthappa P, Densi A, Krishnamurthy RG (2014) Glycogen synthase kinase-β3 in ischemic neuronal death. Curr Neurovasc Res 11(3):271–278. https://doi.org/10.2174/1567202611666140520151002
10. Chuang DM, Wang Z, Chiu CT (2011) GSK-3 as a target for lithium-induced neuroprotection against excitotoxicity in neuronal cultures and animal models of ischemic stroke. Front Mol Neurosci 4:15. https://doi.org/10.3389/fnmol.2011.00015
11. Kelly KL, Ruderman NB (1993) Insulin-stimulated phosphatidylinositol 3-kinase. Association with a 185-kDa tyrosine-phosphorylated protein (IRS-1) and localization in a low-density membrane vesicle. J Biol Chem 268(6):4391–4398. https://doi.org/10.1074/jbc.271.19.11222
12. Frederickson CJ, Koh JY, Bush AI (2005) The neurobiology of zinc in health and disease. Nat Rev Neurosci 6(6):449–462. https://doi.org/10.1038/nrn1671
13. Jiménez-Jiménez FJ, Molina JA, Aguilar MV, Meseguer I, Mateos-Vega CJ, González-Muñoz MJ, de Bustos F, Martínez-Salio A, Ortí-Pareja M, Zurdo M, Martínez-Para MC (1998) Cerebrospinal fluid levels of transition metals in patients with Parkinson's disease. J Neural Transm 105(4–5):497–505. https://doi.org/10.1007/s007020050073
14. Rulon LL, Robertson JD, Lovell MA et al (2000) (2000) Serum zinc levels and Alzheimer's disease. Biol Trace Elem Res 75:79–85. https://doi.org/10.1385/BTER:75:1-3:79
15. Ilouz R, Kaidanovich O, Gurwitz D, Eldar-Finkelman H (2002) Inhibition of glycogen synthase kinase-3beta by bivalent zinc ions: insight into the insulin-mimetic action of zinc. Biochem Biophys Res Commun 295(1):102–106. https://doi.org/10.1016/s0006-291x(02)00636-8
16. Sorci G, Bianchi R, Riuzzi F, Tubaro C, Arcuri C, Giambanco I, Donato R (2010) S100B protein, a damage-associated molecular pattern protein in the brain and heart, and beyond. Cardiovasc Psychiatry Neurol 656481. https://doi.org/10.1155/2010/656481
17. Garg R, Benedetti LG, Abera MB, Wang H, Abba M, Kazanietz MG (2014) Protein kinase C and cancer: what we know and what we do not. Oncogene 33(45):5225–5237. https://doi.org/10.1038/onc.2013.524
18. Arcuri C, Bianchi R, Brozzi F, Donato R (2005) S100B increases proliferation in PC12 neuronal cells and reduces their responsiveness to nerve growth factor via Akt activation. J Biol Chem 280(6):4402–4414. https://doi.org/10.1074/jbc.M406440200
19. Francoz S, Froment P, Bogaerts S, De Clercq S, Maetens M, Doumont G, Bellefroid E, Marine JC (2006) Mdm4 and Mdm2 cooperate to inhibit p53 activity in proliferating and quiescent cells in vivo. Proc Natl Acad Sci USA 103(9):3232–3237. https://doi.org/10.1073/pnas.0508476103
20. Choi YH, Kim SG, Lee MG (2006) Dose-independent pharmacokinetics of metformin in rats: hepatic and gastrointestinal first-pass effects. J Pharm Sci 95(11):2543–2552. https://doi.org/10.1002/jps.20744
21. Patil SP, Jain PD, Ghumatkar PJ, Tambe R, Sathaye S (2014) Neuroprotective effect of metformin in MPTP-induced Parkinson's disease in mice. Neuroscience 277:747–754. https://doi.org/10.1016/j.neuroscience.2014.07.046
22. Wang YW, He SJ, Feng X, Cheng J, Luo YT, Tian L, Huang Q (2017) Metformin: a review of its potential indications. Drug Des Dev Ther 11:2421–2429. https://doi.org/10.2147/DDDT.S141675
23. Arauz-Contreras J, Feria-Velasco A (1984) Monosodium-L-glutamate-induced convulsions—I. Differences in seizure pattern

and duration of effect as a function of age in rats. Gen Pharmacol 15(5):391–395. https://doi.org/10.1016/0306-3623(84)90036-3
24. Peñafiel R, Cremades A, Monserrat F et al (1991) Monosodium glutamate induced convulsions in rats: influence of route of administration, temperature and age. Amino Acids 1:81–89. https://doi.org/10.1007/BF00808094
25. Hinzman JM, Thomas TC, Burmeister JJ, Quintero JE, Huettl P, Pomerleau F, Gerhardt GA, Lifshitz J (2010) Diffuse brain injury elevates tonic glutamate levels and potassium-evoked glutamate release in discrete brain regions at two days post-injury: an enzyme-based microelectrode array study. J Neurotrauma 27(5):889–899. https://doi.org/10.1089/neu.2009.1238
26. McEntee WJ, Crook TH (1993) Glutamate: its role in learning, memory, and the aging brain. Psychopharmacology 111(4):391–401. https://doi.org/10.1007/BF02253527
27. Hanasand M, Omdal R, Norheim KB, Gøransson LG, Brede C, Jonsson G (2012) Improved detection of advanced oxidation protein products in plasma. Clin Chim Acta 413(9–10):901–906. https://doi.org/10.1016/j.cca.2012.01.038
28. Buege JA, Aust SD (1978) Microsomal lipid peroxidation. Methods Enzymol 52:302–310. https://doi.org/10.1016/s0076-6879(78)52032-6
29. Jiang ZY, Hunt JV, Wolff SP (1992) Ferrous ion oxidation in the presence of xylenol orange for detection of lipid hydroperoxide in low density lipoprotein. Anal Biochem 202(2):384–389. https://doi.org/10.1016/0003-2697(92)90122-n
30. Yanar K, Atukeren P, Cebe T, Kunbaz A, Ozan T, Kansu AD, Durmaz S, Güleç V, Belce A, Aydın S, Çakatay U, Rizvi SI (2015) Ameliorative effects of testosterone administration on renal redox homeostasis in naturally aged rats. Rejuvenation Res 18(4):299–312. https://doi.org/10.1089/rej.2014.1640
31. Sun Y, Oberley LW, Li Y (1988) A simple method for clinical assay of superoxide dismutase. Clin Chem 34(3):497–500
32. Aebi H (1984) Catalase in vitro. Methods Enzymol 105:121–126. https://doi.org/10.1016/s0076-6879(84)05016-3
33. Adamo AM, Zago MP, Mackenzie GG, Aimo L, Keen CL, Keenan A, Oteiza PI (2010) The role of zinc in the modulation of neuronal proliferation and apoptosis. Neurotox Res 17(1):1–14. https://doi.org/10.1007/s12640-009-9067-4
34. Seth R, Corniola RS, Gower-Winter SD, Morgan TJ Jr, Bishop B, Levenson CW (2015) Zinc deficiency induces apoptosis via mitochondrial p53- and caspase-dependent pathways in human neuronal precursor cells. J Trace Elem Med Biol 30:59–65. https://doi.org/10.1016/j.jtemb.2014.10.010
35. Abramov AY, Scorziello A, Duchen MR (2007) Three distinct mechanisms generate oxygen free radicals in neurons and contribute to cell death during anoxia and reoxygenation. J Neuroscience 27(5):1129–1138. https://doi.org/10.1523/JNEUROSCI.4468-06.2007
36. Shinohe A, Hashimoto K, Nakamura K et al (2006) Increased serum levels of glutamate in adult patients with autism. Prog Neuropsychopharmacol Biol Psychiatry 30(8):1472–1477. https://doi.org/10.1016/j.pnpbp.2006.06.013
37. Murphy MP (1999) Nitric oxide and cell death. Biochem Biophys Acta 1411(2–3):401–414. https://doi.org/10.1016/s0005-2728(99)00029-8
38. Kirpichnikov D, McFarlane SI, Sowers JR (2002) Metformin: an update. Ann Intern Med 137(1):25–33. https://doi.org/10.7326/0003-4819-137-1-200207020-00009
39. Leng Y, Chuang DM (2006) Endogenous alpha-synuclein is induced by valproic acid through histone deacetylase inhibition and participates in neuroprotection against glutamate-induced excitotoxicity. J Neuroscience 26(28):7502–7512. https://doi.org/10.1523/JNEUROSCI.0096-06.2006
40. Leng Y, Liang MH, Ren M, Marinova Z, Leeds P, Chuang DM (2008) Synergistic neuroprotective effects of lithium and valproic acid or other histone deacetylase inhibitors in neurons: roles of glycogen synthase kinase-3 inhibition. J Neuroscience 28(10):2576–2588. https://doi.org/10.1523/JNEUROSCI.5467-07.2008
41. Cross DA, Culbert AA, Chalmers KA, Facci L, Skaper SD, Reith AD (2001) Selective small-molecule inhibitors of glycogen synthase kinase-3 activity protect primary neurones from death. J Neurochem 77(1):94–102. https://doi.org/10.1046/j.1471-4159.2001.t01-1-00251.x
42. Miranda ER, Dey CS (2004) Effect of chromium and zinc on insulin signaling in skeletal muscle cells. Biol Trace Elem Res 101(1):19–36. https://doi.org/10.1385/BTER:101:1:19
43. Juhaszova M, Zorov DB, Kim SH, Pepe S, Fu Q, Fishbein KW, Ziman BD, Wang S, Ytrehus K, Antos CL, Olson EN, Sollott SJ (2004) Glycogen synthase kinase-3beta mediates convergence of protection signaling to inhibit the mitochondrial permeability transition pore. J Clin Investig 113(11):1535–1549. https://doi.org/10.1172/JCI19906
44. Shin S, Wolgamott L, Yu Y, Blenis J, Yoon SO (2011) Glycogen synthase kinase (GSK)-3 promotes p70 ribosomal protein S6 kinase (p70S6K) activity and cell proliferation. Proc Natl Acad Sci USA 108(47):E1204–E1213. https://doi.org/10.1073/pnas.1110195108
45. Lynch CJ, Patson BJ, Goodman SA, Trapolsi D, Kimball SR (2001) Zinc stimulates the activity of the insulin- and nutrient-regulated protein kinase mTOR. Am J Physiol Endocrinol Metab 281(1):E25–E34. https://doi.org/10.1152/ajpendo.2001.281.1.E25
46. Huang XT, Li C, Peng XP et al (2017) An excessive increase in glutamate contributes to glucose-toxicity in β-cells via activation of pancreatic NMDA receptors in rodent diabetes. Sci Rep 7:44120. https://doi.org/10.1038/srep44120
47. Shen W, Taylor B, Jin Q et al (2015) Inhibition of DYRK1A and GSK3B induces human β-cell proliferation. Nat Commun 6:8372. https://doi.org/10.1038/ncomms9372
48. Domínguez RO, Pagano MA, Marschoff ER, González SE, Repetto MG, Serra JA (2014) Alzheimer disease and cognitive impairment associated with diabetes mellitus type 2: associations and a hypothesis. Neurologia 29(9):567–572. https://doi.org/10.1016/j.nrl.2013.05.006
49. Li DW, Liu ZQ, Chen W, Yao M, Li GR (2014) Association of glycogen synthase kinase-3β with Parkinson's disease (review). Mol Med Rep 9(6):2043–2050. https://doi.org/10.3892/mmr.2014.2080
50. Khallaghi B, Safarian F, Nasoohi S, Ahmadiani A, Dargahi L (2016) Metformin-induced protection against oxidative stress is associated with AKT/mTOR restoration in PC12 cells. Life Sci 148:286–292. https://doi.org/10.1016/j.lfs.2016.02.024
51. Ouslimani N, Peynet J, Bonnefont-Rousselot D, Thérond P, Legrand A, Beaudeux JL (2005) Metformin decreases intracellular production of reactive oxygen species in aortic endothelial cells. Metabolism 54(6):829–834. https://doi.org/10.1016/j.metabol.2005.01.029
52. Zhao RR, Xu XC, Xu F, Zhang WL, Zhang WL, Liu LM, Wang WP (2014) Metformin protects against seizures, learning and memory impairments and oxidative damage induced by pentylenetetrazole-induced kindling in mice. Biochem Biophys Res Commun 448(4):414–417. https://doi.org/10.1016/j.bbrc.2014.04.130